

DISPLACEMENT-BASED SEISMIC DESIGN OF STATICALLY-INDETERMINATE BRIDGE PIERS

Silvia MAZZONI¹ and Gregory L FENVES²

SUMMARY

The development and implementation of a design methodology to estimate structural capacities and demands in seismic design is presented herein. In the methodology, the deformation capacity of a prototype structure is determined from a nonlinear push-over analysis and the displacement demand is calculated from a linear-elastic analysis of a model of the structure. The stiffness and damping characteristics of the linearized model are chosen to represent the inelastic behavior of the structure at a prescribed limit state. The methodology gives the linearized properties directly from the force-deformation behavior determined from the push-over analysis to the limit state. The methodology is unique because it gives local effective stiffnesses associated with the plastic hinge zones. Because the plastic hinge zones have different levels of inelastic response, different stiffness parameters are assigned to the different regions of the nonlinear members. The linearized damping ratio is calculated from the limit-state displacement ductility level. The procedure is implemented for the analysis and design of two-column bridge piers with a flexible cap beam, loaded in the transverse direction of the bridge (in the plane of the pier). The results of this study show that a consistent linearization procedure, which takes into account the stiffness and energy-dissipation characteristics of the structural components locally, can be used for a displacement-based design procedure for bridges.

INTRODUCTION

The development and implementation of a design methodology to estimate structural capacities and demands in seismic design is presented herein. For design purposes, the simplified methodology uses static push-over analyses and elastic dynamic analyses. Nonlinear stiffness reduction and hysteretic energy dissipation (damping) are the primary dynamic characteristics considered in the model.

Current procedures using push-over analysis are typically able to characterize the lateral-deformation capacities and lateral-load strengths of structural systems accurately. Available simplified analysis tools used to calculate the force and deformation demands, however, are limited in their ability to capture the dynamic characteristics of a nonlinear-inelastic prototype in a linear-elastic analysis model.

Because local strains and deformations are considered to be the best indicators of damage, displacement-based design, where member deformation demands and capacities are the primary design parameters, was used as the framework for the proposed procedure. Here, the deformation capacities calculated from a nonlinear static push-over analysis are compared to the deformation demands calculated from a linear-elastic dynamic analysis.

The proposed procedure was implemented in the design and evaluation of a two-column reinforced-concrete bridge bent subjected to vertical gravity loads distributed along the beam length and horizontal seismic ground excitation in the plane of the frame. The bent is shown in Figure 1 and Figure 2. What is particular to the seismic response of bridge structures is that the structural members are designed to have plastic hinges forming at the column ends

¹ Civil & Environmental Engineering, University of California, Los Angeles, CA 90095. Smazzoni@ucla.edu

² Civil & Environmental Engineering, University of California, Berkeley, CA 94720. Fenves@ce.berkeley.edu

rather than in the beams, as is typical in building design. The primary consequence of this design method is that the interaction between the column axial load and flexural strength and stiffness becomes important in the design process. For statically indeterminate systems, the interaction precludes calculating the lateral load strength and deformation capacity directly and independently.

PROPOSED PROCEDURE

In the proposed procedure the lateral-deformation capacity and demand of a structure subjected to the design gravity and seismic loads are calculated and compared. The procedure consists of three phases: the capacity-evaluation phase, the linearization phase, and the demand-evaluation phase. In the capacity-evaluation phase, the structure is subjected to a nonlinear static push-over analysis. The limit-state lateral deflection, together with the local element loads and deformations, are obtained from this analysis. In the linearization phase, a linear-elastic model of the prototype structure is developed from the results of the push-over analysis. The linearized stiffness and damping characteristics are determined in this phase. In the demand-evaluation phase, the linearized model is subjected to the design loads and the lateral-deflection demand is calculated from a linear-elastic dynamic analysis.

CAPACITY EVALUATION PHASE

A nonlinear static push-over analysis is performed on the structure to determine its internal load and deformation characteristics. The calculated lateral-deflection capacity will be compared to the demand calculated in the analysis phase to evaluate the design.

In the static push-over analysis, the portal frame is subjected to simultaneous gravity loads and an incremental lateral deflection at the deck level. The lateral resisting force at the base is determined from a state determination and equilibrium at each deflection increment. The analysis is terminated when the prescribed limit state is reached. At the limit state, a state determination is performed to determine the internal loads and deformations of each structural component. These element loads and deformations are used to calculate the linearization parameters and to determine local demands once the global-response criteria have been satisfied.

Bilinearization of Push-Over Curve

The nonlinear lateral load-deformation response of the prototype structure can be represented by a bilinear approximation, as shown in Figure 3. The bilinear approximation has three defining characteristics. (a) The initial stiffness, K_1 , (b) the maximum load and deformation, F_u and Δ_u , respectively and (c) the second stiffness, K_2 .

The initial elastic stiffness is calculated from a linear-elastic analysis where the flexural stiffness of the members, EI_{cr} , is defined by the ratio of bending moment and the curvature at first yield, M_y and ϕ_y , respectively. First yield for the circular-column elements is defined as the point where the column longitudinal reinforcement first yields in tension, with the dead-load axial force.

The maximum load and deformation at the limit state, F_u and Δ_u respectively, in the bilinear approximation are equal to those of the nonlinear curve. The second stiffness, K_2 , is calculated by equating the strain energy in the nonlinear curve to that in the bilinear approximation, as shown in Figure 4:

$$K_2 = \frac{2F_y\Delta_u K_1 - 2K_1 W_o - F_u^2}{\delta_u^2 K_1 - 2W_o} \quad [1]$$

where the nonlinear work, W_o , can be calculated from integrating the piece-wise-linear force-deformation curve to the limit-state deformation.

Definition of Yield & Ductility

The lateral load, F_y , and lateral deformation, Δ_y , at yield are defined by the intersection of the two stiffnesses in the

bilinear approximation of the push-over response curve:

$$\Delta_y = \frac{F_u - K_2 \Delta_u}{K_1 - K_2} \quad F_y = K_1 \frac{F_u - K_2 \Delta_u}{K_1 - K_2} \quad [2]$$

The yield and limit-state deformations are used to defined the limit-state displacement ductility, μ_Δ :

$$\mu_\Delta = \frac{\Delta_u}{\Delta_y} \quad [3]$$

LINEARIZATION PHASE

In the linearization procedure a linear-elastic model whose dynamic characteristics are representative of those of the nonlinear structure at the limit state is created. The equivalent dynamic characteristics are defined so that the maximum load and deformation demands in the linear-elastic model are the same as those in the nonlinear-inelastic structure.

The nonlinear stiffness reduction and hysteretic energy dissipation characterize the dynamic response of the prototype structure. It is important that the linearization procedure models these two characteristics accurately. To represent the stiffness reduction, the secant stiffness to the limit state is taken as the effective stiffness of the linear-elastic model. The effective viscous damper in the linear-elastic model represents the combined effects of both the viscous damper and the hysteretic-energy dissipation of the prototype structure.

Linearized Stiffness

The development of the proposed procedure is based on the assumption that the structural elements are flexural elements, where only flexural-bending deformations are considered in the modeling. Hence, element stiffness is represented in terms of the section moment of inertia, I . The section moment of inertia is typically characterized in terms of bending-moment and curvature response. Modeling difficulties arise in a yielding system where the nonlinear response of the structural materials results in a reduction in flexural stiffness, EI , with increasing deformation. Where E is the modulus of the material. The modeling of this stiffness reduction when the structure reaches its limit state is the basis of the proposed linearization procedure.

To simplify the analysis procedure, elements that are designed to remain elastic during the response are assumed to remain elastic, as is the case for the beam in the bridge bent. The flexural stiffness typically used for these elastic elements is the cracked-section stiffness, I_{cr} , defined equal to the yield moment divided by the yield curvature and elastic modulus. These quantities can be calculated from a section analysis. Because this stiffness remains constant for any level of deformation and is defined *a priori*, the selection of this stiffness is left to the choice of the designer.

The proposed procedure takes into account the variation of damage in the different structural components by performing a step-by-step static push-over analysis. This step-by-step procedure allows monitoring of all element sections using calculated moment-curvature relationships at the element-section level and follows the sequence of hinge formation. The damage indices for the individual structural elements are determined from the push-over analysis rather than assumed *a priori* and, hence, are particular to each structural element.

In addition, the proposed procedure takes into account the distribution of deformation along the nonlinear structural elements and is able to account for the deformation localization by assigning different stiffness parameters to different regions of the structural elements. The columns in the portal frame considered herein, for example, are subjected to double bending. Based on these boundary conditions, plastic hinges are expected to form at both column ends.

To calculate the linearized-model stiffness characteristics, the element forces (bending moment, shear and axial forces) and nodal deformations (translations and rotations) are extracted from the results of the push-over analysis

at the limit state. These forces and deformations are shown in Figure 5. The linearized model at the limit state is shown in Figure 6. At the limit state, the element forces are the same in the linearized model as those in the nonlinear prototype. To maintain proper modeling of stiffness distribution, the joint translations and rotations are also equal. The difference between the two structural systems lies in the distribution of stiffness along the nonlinear elements. In the prototype structure, the curvature distribution obeys a nonlinear moment-curvature relationship. The resulting curvature along the nonlinear column element is shown in Figure 5.

On the other hand, each column in the linearized model has three segmentally-continuous linear-elastic stiffnesses. The stiffness distribution, and the resulting curvature distribution is shown in Figure 6. Joint rotation and translation impose the two compatibility equations for each nonlinear element necessary to calculate the two end-stiffness parameters, I_a and I_b , shown in Figure 6. The linearized stiffness of the central element, I_o , is assumed constant and equal to the cracked moment of inertia when the column is subjected to the gravity axial force alone and is calculated *a priori*.

The stiffness parameter of each nonlinear element is calculated from its internal forces and deformations. The following equations for the nodal translation, Δ , and the nodal rotation, Θ , shown in Figure 6 are used to determine the stiffness parameters for each column:

$$\Delta = \frac{\frac{1}{6} \frac{b_b^2}{L} (3L - 2b_b) M_b + 2 b_b M_a}{EI_b} + \frac{\frac{1}{6} \frac{b_a}{L} (6L^2 - 6L b_a + 2b_a^2) M_a + (-2b_a^2 + 3L b_a) M_b}{EI_a} + \frac{1}{6} \frac{1}{L} \frac{(-3L b_b^2 + 2b_a^3 + 2b_b^3 + L^3 - 3L b_a^2) M_b + (-2b_b^3 + 2L^3 + 6L b_a^2 - 2b_a^3 - 6L^2 b_a) M_a}{EI_o} \quad [4]$$

$$\Theta = \frac{\frac{1}{2} \frac{b_b}{L} (2L - b_b) M_b + b_b M_a}{EI_b} + \frac{\frac{1}{2} \frac{b_a}{L} (2L - b_a) M_a + b_a M_b}{EI_a} + \frac{1}{2} \frac{1}{L} \frac{(L - b_b - b_a) [(L - b_b + b_a) M_b + (L + b_b - b_a) M_a]}{EI_o} \quad [5]$$

Where L is the length of the element and M_a and M_b are the end moments, as shown in the figure. Solving for the stiffness parameters:

$$EI_a = \frac{A1 \cdot B2 - A2 \cdot B1}{-B3 \cdot A1 + \Theta \cdot A1 - \Delta \cdot B1 + B1 \cdot A3} \quad EI_b = \frac{A1 \cdot B2 - A2 \cdot B1}{B3 \cdot A2 - \Theta \cdot A2 + \Delta \cdot B2 - B2 \cdot A3} \quad EI_o = \frac{M_y}{\phi_y} \Big|_{P_a} \quad [6]$$

Where:

$$\begin{aligned} A1 &= \frac{1}{6} \frac{b_b^2}{L} [(3L - 2b_b) M_b + 2 b_b M_a] \\ A2 &= \frac{1}{6} \frac{b_a}{L} [(6L^2 - 6L b_a + 2b_a^2) M_a + (-2b_a^2 + 3L b_a) M_b] \\ A3 &= \frac{1}{6} \frac{1}{L} \frac{(-3L b_b^2 + 2b_a^3 + 2b_b^3 + L^3 - 3L b_a^2) M_b + (-2b_b^3 + 2L^3 + 6L b_a^2 - 2b_a^3 - 6L^2 b_a) M_a}{EI_o} \end{aligned} \quad [7]$$

and

$$\begin{aligned}
B1 &= \frac{1}{2} \frac{b_b}{L} [(2L - b_b)M_b + b_b M_a] \\
B2 &= \frac{1}{2} \frac{b_a}{L} [(2L - b_a)M_a + b_a M_b] \\
B3 &= \frac{1}{2} \frac{1}{L} \frac{(L - b_b - b_a)[(L - b_b + b_a)M_b + (L + b_b - b_a)M_a]}{EI_o}
\end{aligned} \tag{8}$$

The length of the end segments, b_a and b_b , are additional parameters calculated from the bending moment diagram. The length of these segments is equal to the length over which the bending moment exceeds the yield moment for the section subjected to the dead-load axial force. Based on the graphics of Figure 6, the lengths of the end segments:

$$b_a = \frac{M_a - M_y}{M_a + M_b} L \quad b_b = \frac{M_b - M_y}{M_a + M_b} L \tag{9}$$

The sign convention used in the above expressions is consistent with Figure 5 and Figure 6.

Linearized Damping

The viscous-damping force in the linearized model accounts for the non-conservative forces in the nonlinear prototype: the hysteretic restoring force and the viscous-damping force. The effective damping ratio proposed in this paper was obtained by determining the damping ratio necessary to yield the same maximum demand in the linear-elastic system as in the nonlinear prototype structure. The response of the nonlinear prototype structure was obtained using a nonlinear finite-element analysis program. The input ground motions were selected and scaled so that the maximum demand in the nonlinear prototype was equal to the limit-state deformation obtained in the push-over analysis. The limit state chosen for the implementation procedure was the ultimate limit state, corresponding to the limiting curvature when the extreme compression fiber in the concrete core reaches a strain equal to the maximum strain capacity of the confined concrete. The nonlinear analysis included both the lateral input motion and the gravity load distributed along the beam element. The study was performed using eight unscaled time histories and thirteen frames. An average effective damping ratio was calculated for each frame.

From the results of the study, the linearized damping ratio proposed here is a function of the characteristics of the linearized push-over curve:

$$\zeta_{eff} = \frac{1}{\pi} \left(1 - \frac{1 - \alpha}{\sqrt{\mu_{\Delta}}} - \alpha \sqrt{\mu_{\Delta}} \right) + \zeta_o \tag{10}$$

The displacement-ductility factor, μ_{Δ} , is defined above and the stiffness ratio α is equal to the ratio of the second stiffness to the initial stiffness, as derived above and shown in Figure 3:

$$\alpha = \frac{K_2}{K_1} \tag{11}$$

ζ_o is the viscous-damping ratio of the nonlinear system. This relationship was obtained by equating the one-cycle hysteretic energy from an analytical force-deformation model for reinforced concrete to the one-cycle energy of the effective viscous damper. The Takeda force-deformation response model was used for the hysteretic modeling.

The above expression for the effective damping ratio was developed for structures whose linearized natural period ranged between 1.0 and 3.2 seconds. The displacement-ductility range was between 2 and 6.2.

DEMAND-ANALYSIS PHASE

In the analysis phase, the linearized system, with effective stiffnesses and an effective damping ratio is subjected to the design loads – seismic and gravity. The portal frame under consideration in the implementation of the procedure can be reduced to an SDOF system, taking both types of loads into account, through static condensation of the stiffness matrix. The natural frequency of the system, ω_n , is calculated from this static condensation. When gravity bending moments are accounted for, the linearized stiffness is not equal to the limit-state force divided by the displacement at the limit state. In the analysis, the gravity forces must be included and are calculated in the static condensation.

RESULTS

The procedure presented in this paper was implemented in the design and analysis of a portal frame whose design characteristics are within the range used in the development of the methodology, but are not identical to any particular frame. A different set of eight time histories was used in the analysis and 5% viscous damping was included in the nonlinear system.

A pushover analysis of the portal frame was performed to determine (a) the lateral load and deformation response characteristics and (b) the internal loads and deformations necessary to determine the linearized stiffness characteristics. The limit-state load and deformation, F_u and Δ_u , for the portal frame were calculated to be 1218 kips and 15.7 inches, respectively. The initial and secondary stiffnesses, K_1 and K_2 , were calculated to be 138.3 and 41.5 kip/inch, respectively. The corresponding yield force and deformation, F_y and Δ_y , were calculated to be 810 kip and 5.9 inches, respectively, with a displacement-ductility capacity of 2.7. The push-over envelope for the test structure is shown in Figure 7.

The natural period of the linearized structure was calculated to be 1.8 seconds. The damping ratio of the linearized structure, including the 5% viscous damping, was calculated to be 10.1%. The mass of the system, corresponding to a column axial load of 6% of its gross capacity, was 2.7×10^6 lb-mass. Using these properties, the linearized system was subjected to eight ground motions, scaled to correspond to the prescribed limit state..

To assess the validity of the methodology, the response of the linearized system was compared to the response of the nonlinear prototype subjected to the same input ground motion. These two responses are compared in Figure 8. This figure corresponds to the response to the Tabas ground motions in the X direction, scaled by a factor of 1.253.

The ratio of maximum elastic-deformation demand to maximum nonlinear-deformation demand was calculated for each time history. The mean and standard deviation for all eight time histories were calculated to be 1.06 and 12.7%, respectively.

CONCLUSIONS

The implementation of the methodology to the analysis and design of a test frame has shown that proposed procedure yields promising results. The linearization procedure is two-fold. First, the stiffness linearization is based on the physical response of the structural components and can be extended to MDOF systems. The estimating of the effective damping ratio is based on a rigorous analytical study and takes into account more structural characteristics than the displacement ductility alone.

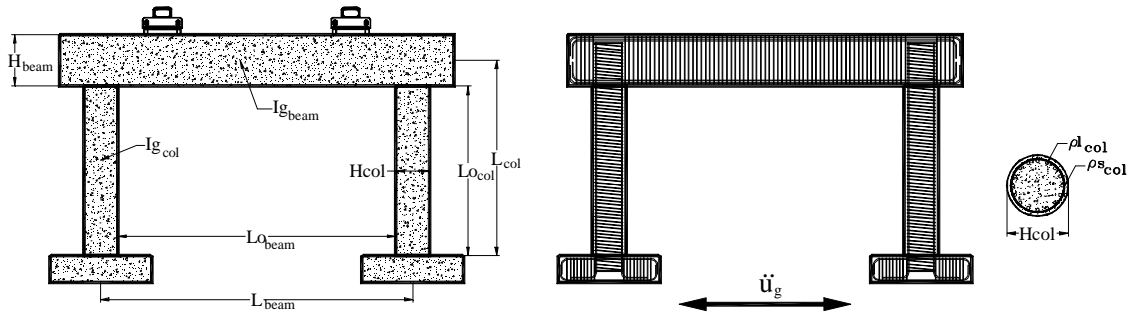


Figure 2. Two-Column Reinforced-Concrete Bridge Bent

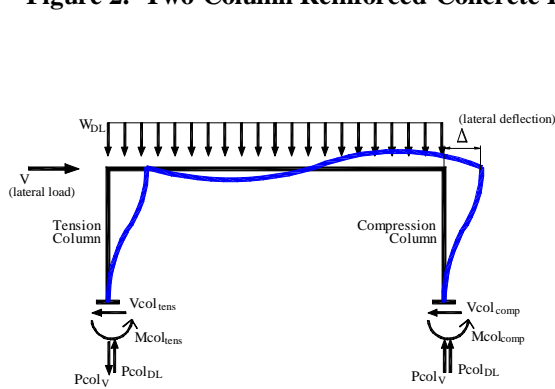


Figure 3. Lateral & Gravity Loads, Support Reactions, and Lateral Deflection of Portal Frame

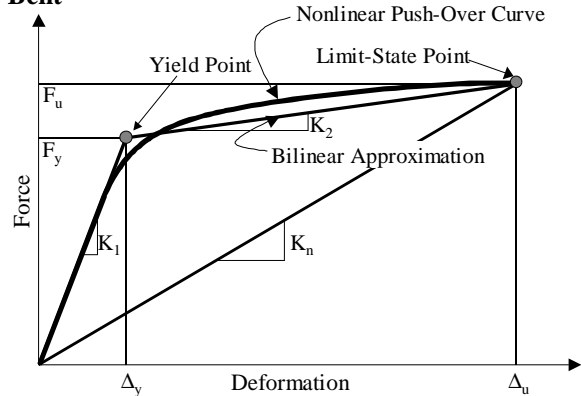
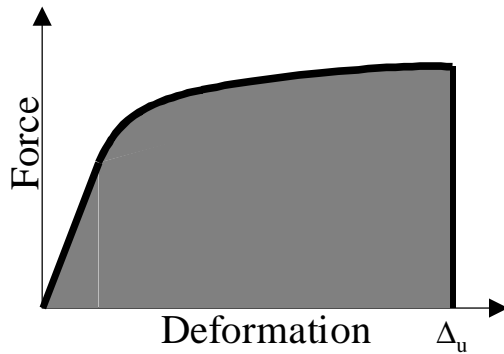
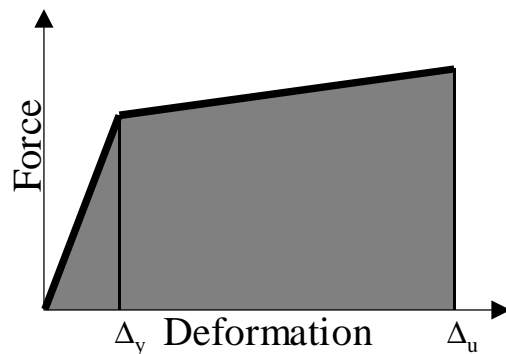


Figure 4. Bilinearization of Nonlinear Push-Over Curve

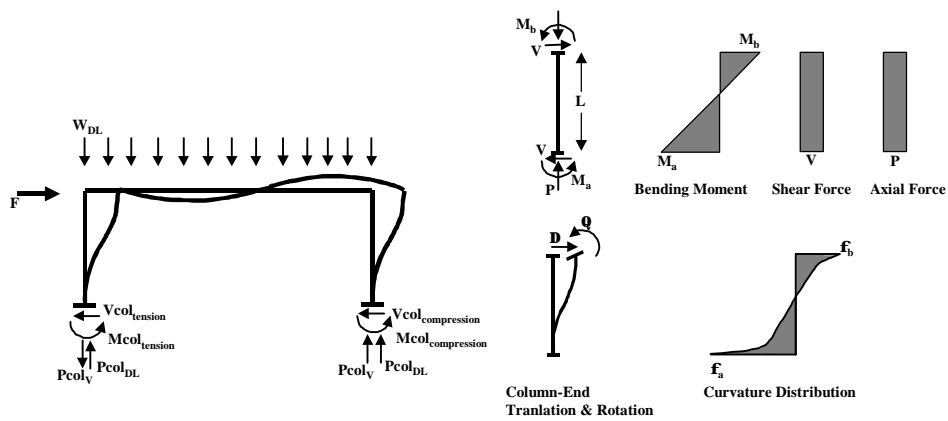


(a) nonlinear curve



(b) bilinear approximation

Figure 5. Strain/Deformation Energy in Push-Over Curves



SYSTEM FORCES & DEFORMATIONS

COLUMN FORCES & DEFORMATIONS

Figure 6. Element Forces and Deformations in Nonlinear Members

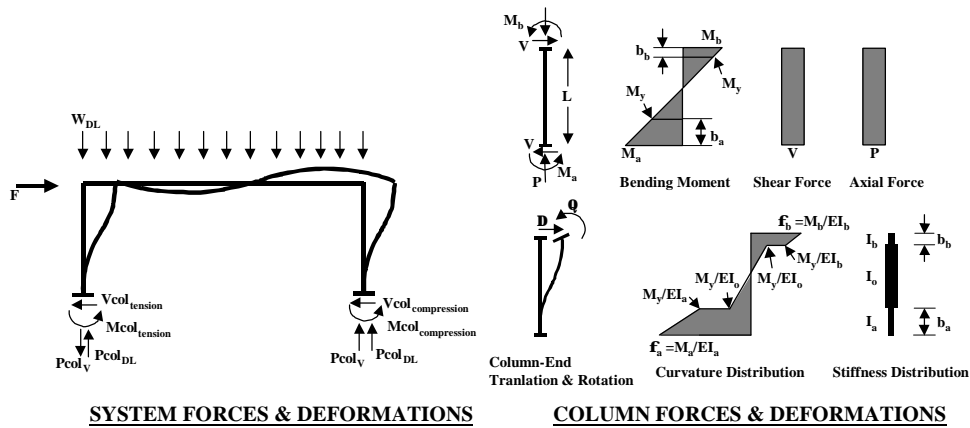


Figure 7. Element Forces and Deformations in Linearized Members

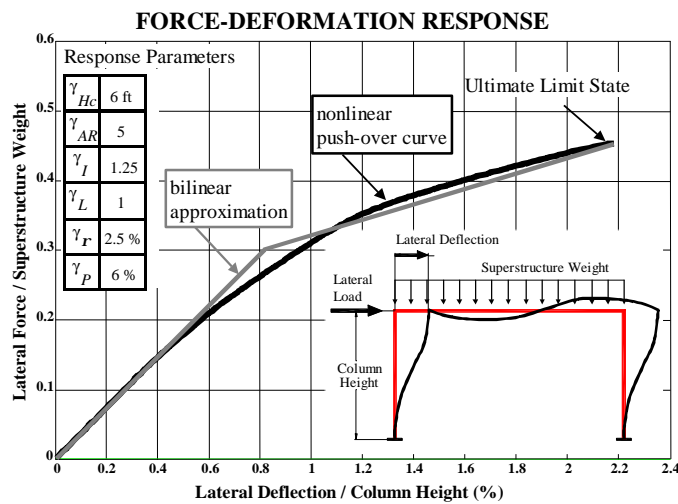


Figure 8. Push-Over Curve of Test Structure

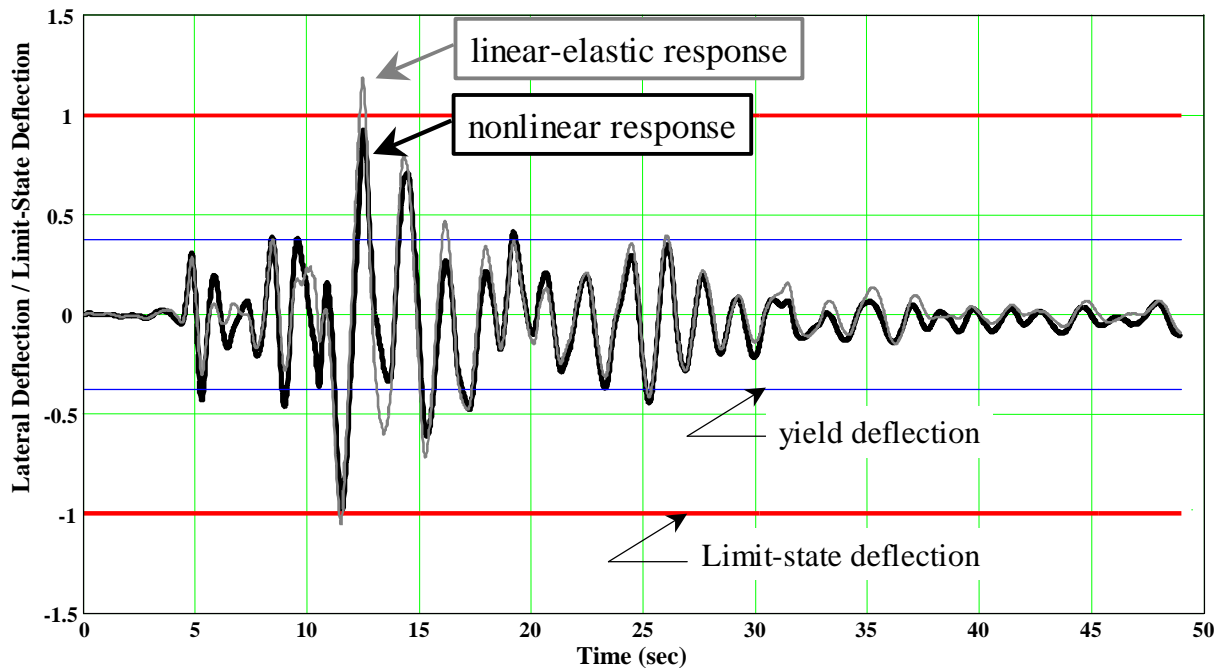


Figure 9. Time-History Response of Nonlinear and Linearized Test Structure. Tabas X-Direction.